Macromolecules

Article

pubs.acs.org/Macromolecules

Nonlinear Elasticity: From Single Chain to Networks and Gels

Jan-Michael Y. Carrillo,[†,‡] Fred C. MacKintosh,[§] and Andrey V. Dobrynin*[,†]

[†]Polymer Program, Institute of Materials Science and Department of Physics, University of Connecticut, Storrs, Connecticut 06269, United States

[‡]Scientific Computing Department, National Center for Computational Sciences, Oak Ridge National Laboratories, Oak Ridge, Tennessee 37831, United States

[§]Department of Physics and Astronomy, VU University, Amsterdam 1081 HV, The Netherlands

ABSTRACT: Biological and polymeric networks show highly nonlinear stress−strain behavior manifested in materials that stiffen with increasing deformation. Using a combination of the theoretical analysis and molecular dynamics simulations, we develop a model of network deformation that describes nonlinear mechanical properties of networks and gels by relating their macroscopic strain-hardening behavior to molecular parameters of the network strands. The starting point of our approach is a nonlinear force/elongation relation for discrete chains with varying bending rigidity. The derived expression for the network free energy is a universal function of the first deformation invariant and chain elongation ratio that depends on a ratio of the unperturbed chain size to chain dimension in a fully extended conformation. The model predictions for the nonlinear shear modulus and differential shear modulus for uniaxial and shear deformations are in very good agreement with both the results of molecular dynamics simulations of networks and with experimental data for biopolymer networks of actin, collagen, fibrin, vimentin, neurofilaments, and pectin.

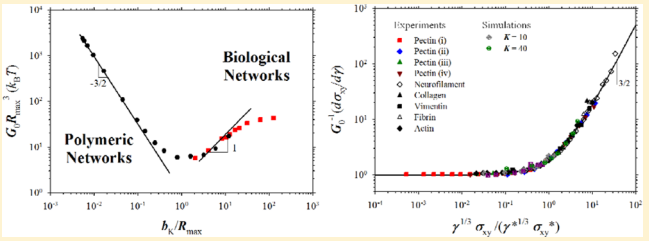

INTRODUCTION

Networks are important structural components of automotive tires,[1] paper,[2] living cells,[3−5] and tissues.[6−9] These materials demonstrate unique mechanical properties. For example, a natural rubber and synthetic polymeric networks can be reversibly deformed at applied stresses on the order of 10^4−10^7 Pa and sustain deformations up to 10 times of their initial size.[1,10−12] The biological networks of actin and collagen are deformed at much low external stresses 10^{-1}−10^2 Pa that require shear strains, $\gamma \leq 1$.[7,13−19] Such dramatic difference in behavior of polymeric and biological networks is a reflection of difference in the elastic response of individual macromolecules or filaments comprising the networks. In polymeric networks chains are highly coiled such that their extension results in reduction of the number of available chain conformations. Therefore, the elastic response of these networks is entropic in nature.[1,20] In biological networks, filaments of a network are almost fully extended between cross-links. For such networks, their deformation can involve both filament's bending[21,22] and stretching, where the latter can be either entropic[23] or enthalpic in nature.[18,24] Molecular models of network elasticity based on deformation of individual network strands treat polymeric and biological networks as two different classes of soft-elastic materials.[1,18,20,24−27]

It was shown recently that deformation of both polymeric and biological macromolecules can be described by a discrete chain model with a bending constant K in the entire interval of chain deformations (see Figure 1).[28] According to this model a polymeric chain behaves as a worm-like chain (WLC) under tension in the interval of the applied forces f smaller than the crossover force f_c. Magnitude of the crossover force $f_c \propto Kk_BT/b$ depends on the effective chain bending constant K (or chain Kuhn length b_K) and bond length b (k_B is the Boltzmann constant, and T is the absolute temperature). In the nonlinear chain deformation regime, $f < f_c$, an applied force demonstrates a quadratic divergence, $f \propto (R_{max} - R)^{-2}$, as a size of the deformed

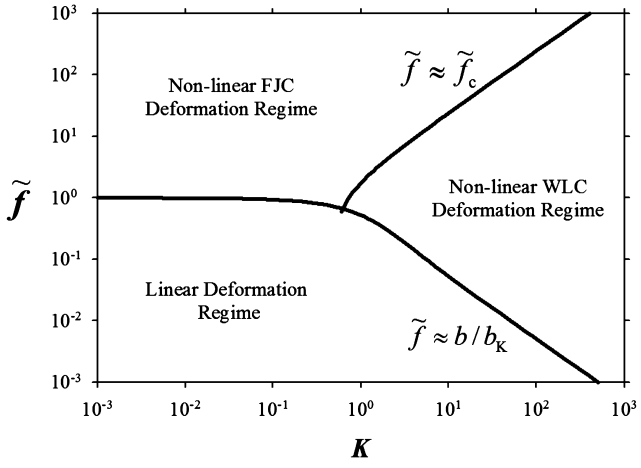

Figure 1. Diagram of different chain deformation regimes. $\tilde{f} = fb/k_BT$ is a reduced force. Solid lines represent crossover between different chain deformation regimes and are given by $\tilde{f}_c \approx 2.47\,K(1 - 0.5/K)^{1/2}$ and $\tilde{f} \approx b/b_K = (1 - \coth(K) + K^{-1})/(1 + \coth(K) - K^{-1})$.

Received: March 5, 2013
Published: April 26, 2013

chain R approaches its fully extended size, R_{max}.[20,29] This quadratic divergence is a characteristic feature of deformation of biological macromolecules (worm-like chains), both for chain segments longer than the chain persistence length[30−32] and for chain segments shorter that the persistence length (e.g., for cytoskeletal biopolymers).[23] This divergence is associated with the pulling out chain's transverse bending deformation modes. However, in the interval of the external forces f exceeding the crossover force, $f > f_c$, the chain tension diverges as $f \propto (R_{max} - R)^{-1}$ (see Figure 1). This is usually the case for flexible chains described by the freely jointed chain (FJC) model[20] and is manifestation of the finite chain extensibility.

Here, we present a nonlinear network deformation model based on the discrete chain model with bending rigidity K that allows us to describe both polymeric and biological networks in the framework of the unified network deformation model. As in the case of individual chain stretching, a combination of entropic stretching and bending deformation modes control the elastic response of networks. This is manifested in different dependences of the nonlinear network shear modulus on network deformation. We verified predictions of the nonlinear network deformation model by molecular dynamics simulations and compared them with experimental results for biological networks and gels.

NONLINEAR NETWORK DEFORMATION MODEL

A starting point for our derivation of the network free energy is nonlinear force−extension relation between applied force f and the average distance between chain ends $\langle R\rangle$ along the force direction.[28] For a discrete model of a chain with bending constant K and the number of bonds N_b this relation is written as follows

$$\frac{f}{k_BT} \approx \frac{3\langle R\rangle}{\langle R_0^2\rangle} + \frac{2\langle R\rangle}{R_{max}b}\left[\sqrt{K^2 + (1 - \langle R\rangle^2/R_{max}^2)^{-2}} - \sqrt{K^2+1}\right] \quad (1)$$

where k_B is the Boltzmann constant, T is the absolute temperature, $R_{max} = bN_b$ is a length of the fully extended chain with the bond length b, and $\langle R_0^2\rangle \approx b_K R_{max}$ is the mean-square average end-to-end distance of an ideal chain with the Kuhn length b_K.

$$b_K = b\frac{1 + \coth(K) - K^{-1}}{1 - \coth(K) + K^{-1}} \approx \begin{cases} 2bK, & \text{for } K >> 1 \\ b, & \text{for } K << 1 \end{cases} \quad (2)$$

This expression (eq 1) for the chain deformation as a function of the applied force covers both linear and nonlinear chain deformation regimes. In the force interval $f \le k_BT/b_K$, eq 1 reproduces a linear relation between the chain deformation and magnitude of the applied force, $\langle R\rangle \propto f b_K R_{max}/k_BT$ (see Figure 1). In the nonlinear chain deformation regime $k_BT/b_K \le f$, there are two different regimes of chain deformation and the crossover between these two regimes depends on the chain bending rigidity (see Figure 1). Polymer chains with bending constant $K > 1$ behave as a worm-like chain under tension in the interval of the applied forces $f \le Kk_BT/b$ and as a freely jointed chain for $f \ge Kk_BT/b$.

In deriving expression for network free energy, we will use a mean-field approximation and assume that chain end-to-end distance $R \approx \langle R\rangle$ in eq 1. The dependence of the chain's free energy on the chain end-to-end distance R is obtained by using principle of virtual work and by considering eq 1 as an equation describing force-deformation relationship of a nonlinear spring with the spring length R.[33] The chain's free energy is calculated as a work done by stretching a chain (nonlinear spring) by a constant force f pointing along the end-to-end vector $\vec{R}$ by a distance $d\vec{R}$

$$dF = [\vec{f}(R)\cdot d\vec{R}] = f(R)\, dR \quad (3)$$

Performing integration over R, one obtains

$$\frac{F(R)}{k_BT} \approx \frac{3R^2}{2\langle R_0^2\rangle} - \frac{R_{max}}{b}g\left(K\left(1 - \frac{R^2}{R_{max}^2}\right)\right) - \frac{R^2}{R_{max}b}\sqrt{K^2+1} \quad (4)$$

where we defined function $g(x)$ as follows

$$g(x) = \sqrt{1+x^2} + \frac{1}{2}\log\left[\frac{\sqrt{1+x^2} - 1}{\sqrt{1+x^2} + 1}\right] \quad (5)$$

Note that in the limit of small chain deformations, $R/R_{max} << 1$, eq 4 reproduces the elastic free energy of an ideal chain. Thus, our expression for the chain's free energy eq 3 can be considered as an extension of the elastic free energy of an ideal chain to the case of nonlinear chain deformations.

Let us assume that a network is isotropic and cross-links connecting polymeric strands have $N = N_b + 1$ monomers each. In the framework of the affine network deformation model each strand undergoes an affine deformation[1,20] such that $R_s^x = \lambda_x R_{in}^x$, $R_s^y = \lambda_y R_{in}^y$, and $R_s^z = \lambda_z R_{in}^z$, and the free energy of a network is equal to the sum of contributions from individual strands between cross-links.

$$F_{net}(\{\lambda_i\}) = \sum_s F(R_s) \approx GV\left(\frac{I_1(\{\lambda_i\})}{2} - \frac{b_K}{b\beta}g\left(K\left(1 - \frac{\beta I_1(\{\lambda_i\})}{3}\right)\right) - \frac{I_1(\{\lambda_i\})}{3}\frac{b_K\sqrt{K^2+1}}{b}\right) \quad (6)$$

where V is the system volume, $I_1(\{\lambda_i\}) = \lambda_x^2 + \lambda_y^2 + \lambda_z^2$ is the first strain invariant of the deformation matrix, and $\langle R_{in}^2\rangle$ is the mean-square end-to-end distance of a strand between cross-links in the undeformed network,

$$G \approx k_BT\frac{\rho}{N}\frac{\langle R_{in}^2\rangle}{\langle R_0^2\rangle} \quad (7)$$

is the shear modulus of the network with monomer density ρ. $\beta = \langle R_{in}^2\rangle/R_{max}^2$ is the ratio of the mean-square distance between cross-links in the undeformed network and the square of the end-to-end distance of the fully extended strand. This parameter determines how much a polymeric strand between cross-links can be stretched. In deriving eq 6 we have assumed an affine deformation of the network strands such that $\langle R_s^2\rangle = I_1(\{\lambda_i\})\langle R_{in}^2\rangle/3$ and used a preaveraging approximation substituting $\langle g(1 - x^2)\rangle$ by $g(1 - \langle x^2\rangle)$. It is important to point out that the accuracy of the preaveraging approximation improves when the value of the parameter $x \approx 1$ and $x << 1$. In the case $x \approx 1$, the fluctuations δx around the average value are small, $\delta x/\langle x\rangle << 1$, such that $\langle x^2\rangle \approx \langle x\rangle^2 \approx x^2$. In the opposite limit, when $x << 1$, we can use the following approximation $\langle g(1 - x^2)\rangle \approx g(1) - g'(1)\langle x^2\rangle$. Advantage of using eq 6 is that it allows us to

dx.doi.org/10.1021/ma400478f | Macromolecules 2013, 46, 3679−3692

describe elasticity of a network using only two adjustable parameters: the network shear modulus G and the chain elongation ratio β.

We apply eq 6 to describe nonlinear stress−strain relation in a network undergoing uniaxial and shear deformations. For the uniaxial deformation at a constant volume the product of the deformation (elongation) ratios is a constant $\lambda_x\lambda_y\lambda_z = 1$, such that the network extends in one direction and contracts in two others resulting in $\lambda_x = \lambda$; $\lambda_y = \lambda_z = 1/\lambda^{1/2}$. The true (physical) stress generated in the uniaxially deformed network is equal to

$$\sigma_{xx}(\lambda) = \frac{\lambda}{V}\frac{\partial F_{net}(\lambda)}{\partial \lambda} = \frac{G}{3}(\lambda^2 - \lambda^{-1}) \left(3 + \frac{2b_K}{b}\sqrt{K^2 + \left(1 - \frac{\beta I_1(\lambda)}{3}\right)^{-2}} - \frac{2b_K}{b}\sqrt{K^2 + 1}\right) \quad (8)$$

where the first strain invariant for the uniaxially deformed network is $I_1(\lambda) = (\lambda^2 + 2/\lambda)$.

For a shear the three principal extension ratios are $\lambda_1 = \lambda$, $\lambda_2 = 1/\lambda$, and $\lambda_3 = 1$.[1] It is important to point out that the direction of the principle axes of strain are not related to the direction of shear in any simple way and depend on the magnitude of the strain. The shear strain γ is equal to $\gamma = \tan\phi = \lambda - \lambda^{-1}$[1] and the shear stress generated in the deformed network is equal to

$$\sigma_{xy}(\gamma) = \frac{1}{V}\frac{\partial F_{net}(\gamma)}{\partial \gamma} = \frac{G\gamma}{3} \left(3 + \frac{2b_K}{b}\sqrt{K^2 + \left(1 - \frac{\beta I_1(\gamma)}{3}\right)^{-2}} - \frac{2b_K}{b}\sqrt{K^2 + 1}\right) \quad (9)$$

where the first strain invariant for the shear deformation is $I_1(\gamma) = \gamma^2 + 3$.

Thus, eqs 8 and 9 describe network deformation in both linear and nonlinear deformation regimes. In the linear deformation regime the value of the parameter $\beta I_1/3$ is much smaller than unity such that

$$\sigma_{xx}(\lambda) \approx G(\lambda^2 - \lambda^{-1}), \quad \text{for } \beta I_1 < 1 \quad (10)$$

It is important to point out that for this regime to exist it is necessary for the value of the parameter β to be much smaller than unity, $\beta \ll 1$. For such networks, the value of $\langle R_{in}^2\rangle \approx \langle R_0^2\rangle \approx b_K R_{max}$ and there are many Kuhn segments per network strand, $R_{max} \gg b_K$. This is usually the case for polymeric networks. In this regime network shear modulus at small deformations G_0 is defined as

$$G_0 \equiv \left.\frac{\sigma_{xx}(\lambda)}{\lambda^2 - \lambda^{-1}}\right|_{\lambda=1} = G, \quad \text{for } \beta I_1 < 1 \quad (11)$$

It follows from this equation that shear modulus G coincides with the shear modulus at small deformations G_0 and is on the order of the thermal energy k_BT per network strand

$$G_0 \approx G \propto k_B T\rho/N \quad (12)$$

The elastic response of polymeric networks is controlled by entropic elasticity (entropic stretching) of the individual network strands. Therefore, we can associate the shear modulus G with stretching deformation mode of the strands between cross-links and call this regime the "Entropic Stretching Regime" in the diagram of network deformation regimes shown in Figure 2. In this regime, network shear modulus at small deformations

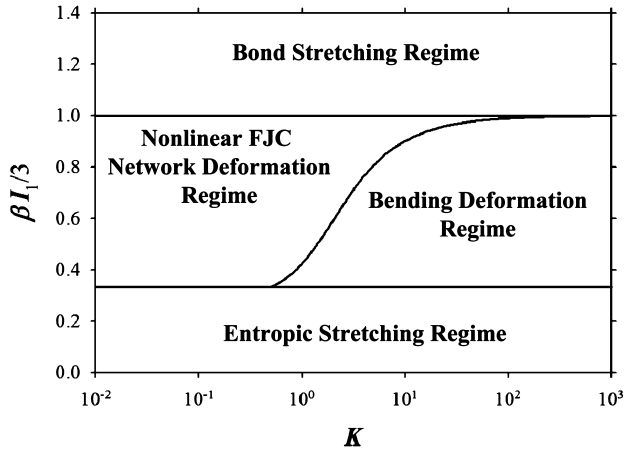

Figure 2. Diagram of different network deformation regimes.

$$G_0 \approx G \approx k_B T\frac{\rho}{N} \approx k_B T(b_K R_{max})^{-3/2} \quad (13)$$

decreases with increasing the chain Kuhn length b_K. In derivation of eq 13, we substituted for monomer concentration $\rho \approx N/(b_K R_{max})^{3/2}$.

A crossover from entropic chain stretching to chain bending deformation mode for polymer chains with $K > 1$ occurs at $K(1 - \beta I_1/3) > 1$. In this network deformation regime, expression 8 reduces to

$$\sigma_{xx}(\lambda) \approx \frac{G}{3}(\lambda^2 - \lambda^{-1})\left[1 + 2\left(1 - \frac{\beta I_1}{3}\right)^{-2}\right], \quad \text{for } K(1 - \beta I_1/3) > 1 \quad (14)$$

where we take into account that $b_K \approx 2Kb$. This regime is called the "Bending Deformation Regime" in Figure 2. In this deformation regime eqs 8 and 9 are identical to the ones derived in our previous publication and describe deformation of the networks made of worm-like chains (WLC networks).[33] The bending deformation regime corresponds to nonlinear deformations of networks made from long polymeric strands with chain elongation ratio $\beta \ll 1$ or $\langle R_{in}^2\rangle \approx b_K R_{max} \ll R_{max}^2$ (polymeric networks). In the case of networks made from short rigid chains between cross-links (biological networks) with $R_{max} \ll b_K$, ($\beta \approx 1$) this regime occurs at small network deformations, $\lambda \approx 1$. The shear modulus of biological networks at small deformations, G_0, is equal to

$$G_0 \equiv \left.\frac{\sigma_{xx}(\lambda)}{(\lambda^2 - \lambda^{-1})}\right|_{\lambda=1} \approx \frac{2G}{3(1 - \beta)^2}, \quad \text{for } K(1 - \beta) > 1 \quad (15)$$

In biological networks strands between cross-links are almost fully stretched such that[20]

$$\langle R_{in}^2\rangle = 2b^2K^2\left(\frac{N}{K} - 1 + \exp\left(-\frac{N}{K}\right)\right) \underset{N\ll K}{\approx} R_{max}^2\left(1 - \frac{2R_{max}}{3b_K}\right) \quad (16)$$

dx.doi.org/10.1021/ma400478f | Macromolecules 2013, 46, 3679−3692

Therefore, network shear modulus G reduces to $G \propto k_BT(\rho/N)R_{max}/b_K$. Taking this into account and using eq 16 for evaluation of the parameter β we obtain[18]

$$G_0 \approx \frac{3}{2}\frac{Gb_K^2}{R_{max}^2} \approx \frac{3}{2}k_BT\frac{b_K}{R_{max}^4} \approx E_{bend}\rho^2 b^3 \quad (17)$$

where we substituted for monomer concentration $\rho^{-1} \approx bR_{max}^2$. Equation 17 confirms that for networks made from stiff chains (or filaments) the main contribution to the network shear modulus G_0 comes from strand bending rigidity and shear modulus is proportional to the bond bending energy, $E_{bend} = k_BTK$. In a polymer chain bonds are connected in series resulting in the net bending energy of a chain being N times smaller than bending energy of a bond, $E_{bend}^{ch} = E_{bend}/N$. Therefore, the network shear modulus G_0 is on the order of chain bending energy $E_{bend}^{ch} = k_BTb_K/R_{max}$ per volume occupied by a polymeric strand between cross-links, R_{max}^3 (see eq 17).

In the range of network deformations such that $K(1 - \beta I_1/3) \ll 1$, the network stress shows a hyperbolic divergence as a function of the network deformation parameter $(1 - \beta I_1/3)$.

$$\sigma_{xx}(\lambda) \approx \frac{2Gb_K}{3b}(\lambda^2 - \lambda^{-1})\left(1 - \frac{\beta I_1(\lambda)}{3}\right)^{-1}, \quad \text{for } K(1 - \beta I_1/3) \ll 1 \quad (18)$$

This divergence of the stress is a characteristic feature of the networks made of freely jointed chains (FJC networks). Thus, at a very large network deformations even networks made of polymeric chains with finite bending rigidity behave as FJC networks. This is in agreement with the behavior of the polymer chains with finite bending rigidity under applied external force (see Figure 1 and ref 28 for details). A more accurate location of the crossover between the bending deformation regime and the nonlinear FJC network deformation regime that is correct for an arbitrary chain bending constant K is obtained by using the following representation of the nonlinear term in eqs 8 and 9

$$\sqrt{K^2 + \left(1 - \frac{\beta I_1(\lambda)}{3}\right)^{-2}} \approx \sqrt{K^2 + 1}\left(1 + \frac{1}{(K^2+1)}\left[\left(1 - \frac{\beta I_1(\lambda)}{3}\right)^{-2} - 1\right]\right)^{1/2} \quad (19)$$

Therefore, a crossover between these two regimes occurs at

$$\frac{\beta I_1}{3} \approx 1 - (K^2 + 2)^{-1/2} \quad (20)$$

For flexible chains with $K \ll 1$, there is a direct crossover from the entropic stretching regime to the nonlinear FJC network deformation regime (see Figure 2). Note that for networks made from nonextensible polymer chains the value of the deformation parameter, $\beta I_1/3$, can not exceed unity, $\beta I_1/3 < 1$. However for real polymeric networks at very large network deformations one can expect deformation of the individual strand's bonds and bond angles. This network deformation regime is shown as "Bond Stretching Regime" in Figure 2. In the bond stretching regime network elastic properties are similar to those of the mechanical network.[26,27] It is also worth pointing out that for very stiff networks with bending constant $K \geq 10^3$ and $R_{max} \ll b_K$ the crossover between bending and bond stretching deformation regimes should bear similarities with a similar crossover in three-dimensional fiber networks.[26,27]

COMPARISON WITH SIMULATION RESULTS

Network Deformation and Shear Modulus. To establish how well our network deformation model describes deformation of networks made of flexible and semiflexible chains we have performed molecular dynamics simulations of deformation of diamond networks. The simulation details are described in Appendix A. Parts a and b of Figures 3 show our simulation results for uniaxial network deformation as a function of the network deformation ratio λ. The lines on these figures correspond to a best fit to the eq 8 with two fitting parameters: network shear modulus G and chain elongation ratio β. The values of the fitting parameters are listed in Table 1. It follows from these figures that eq 8 describes our simulation data reasonably well in the wide interval of the network deformation ratios. The deviation from eq 8 is observed for long stiff polymer chains (see Figure 3 a data points for $K > 0.125$) and for all data sets of short polymer chains shown in Figure 3b. This deviation is due to bond stretching. In this deformation regime network elasticity is controlled by the elastic response of the individual bonds. Note that the crossover to bond stretching regime takes place for stiff chains at smaller values of the network deformation ratio. This should not be surprising since the stiffer polymer

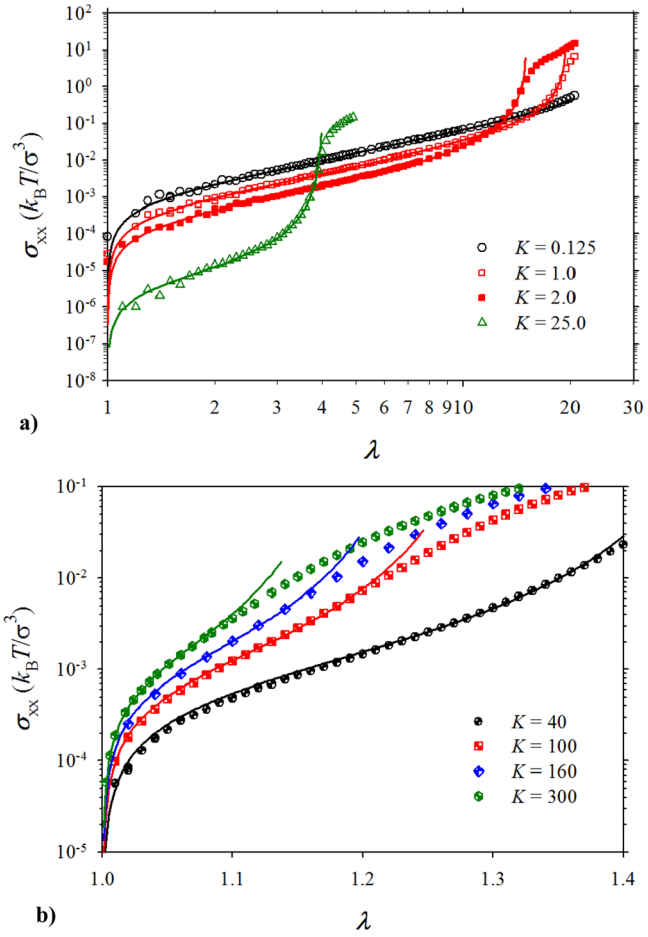

Figure 3. Dependence of the network stress σ_{xx} on deformation ratio λ for diamond networks consisting of polymer chains with different values of the bending constant K and number of monomers $N = 200$ (a) and $N = 20$ (b).

dx.doi.org/10.1021/ma400478f | Macromolecules 2013, 46, 3679−3692

Table 1. Values of the Fitting Parameters for Diamond Networks with the Number of Monomers $N = 20$ and $N = 200$

$N = 20$					
K	b_K/b	b_K/R_{max}	G (k_BT/σ^3)	β_{fit}	β_{sim}
20	39	2.05	1.12×10^{-4}	0.739	0.796 ± 0.094
40	79	4.16	5.36×10^{-5}	0.852	0.890 ± 0.056
80	159	8.37	3.08×10^{-5}	0.916	0.943 ± 0.031
100	199	10.47	2.06×10^{-5}	0.934	0.953 ± 0.025
120	239	12.58	1.73×10^{-5}	0.944	0.961 ± 0.022
160	319	16.79	1.49×10^{-5}	0.953	0.970 ± 0.018
200	399	21.00	9.35×10^{-6}	0.965	0.976 ± 0.015
300	599	31.53	7.59×10^{-6}	0.972	0.983 ± 0.012
600	1199	63.11	5.48×10^{-6}	0.978	0.990 ± 0.010
1200	2399	126.26	5.00×10^{-6}	0.980	0.995 ± 0.005
$N = 200$					
K	b_K/b	b_K/R_{max}	G (k_BT/σ^3)	β_{fit}	β_{sim}
0.125	1.09	0.005	5.98×10^{-4}	0.0045	0.007 ± 0.005
0.25	1.18	0.006	5.26×10^{-4}	0.0050	0.008 ± 0.005
0.5	1.39	0.007	4.08×10^{-4}	0.0059	0.009 ± 0.006
1	1.91	0.010	2.61×10^{-4}	0.009	0.012 ± 0.008
2	3.32	0.017	1.16×10^{-4}	0.013	0.021 ± 0.013
5	9.00	0.045	2.62×10^{-5}	0.036	0.056 ± 0.034
10	19.00	0.10	8.40×10^{-6}	0.075	0.115 ± 0.067
15	29.00	0.15	4.55×10^{-6}	0.111	0.171 ± 0.094
25	49.00	0.25	2.14×10^{-6}	0.181	0.266 ± 0.130
40	79.00	0.40	1.10×10^{-6}	0.279	0.383 ± 0.157
80	159.00	0.80	4.10×10^{-7}	0.482	0.518 ± 0.147
160	319.00	1.60	1.63×10^{-7}	0.681	0.693 ± 0.105
320	639.00	3.21	6.74×10^{-8}	0.803	0.812 ± 0.078
600	1199.00	6.03	2.70×10^{-8}	0.894	0.914 ± 0.045
1200	2399.00	12.06	1.43×10^{-8}	0.943	0.958 ± 0.022

chains are the closer they are to the fully extended chain conformation in undeformed networks, $\lambda = 1$. For such networks the chain elongation ratio β varies between 0.7 and 0.98.

We can use our simulation results to verify a scaling dependence of the network shear modulus on the system parameters (see eq 7)

$$G \approx k_BT\frac{\rho}{N}\frac{\langle R_{in}^2\rangle}{\langle R_0^2\rangle} \approx k_BT\rho\beta\frac{b}{b_K} \quad (21)$$

In simplifying the last equation we substituted for $\langle R_{in}^2\rangle \approx \beta R_{max}^2 \approx \beta b^2N^2$, and $\langle R_0^2\rangle \approx b_K R_{max}$. Therefore, the reduced network shear modulus $G/(k_BT\rho\beta)$ is proportional to the ratio of the bond length to the Kuhn length, b/b_K. This is plotted in Figure 4. The network shear modulus decreases with increasing the chain bending rigidity or chain Kuhn length b_K.

Before discussing nonlinear network elasticity we will consider linear network deformation. Dependence of the network shear modulus G_0 at small deformations on the ratio of b_K/R_{max} is shown in Figure 5. For polymeric networks with $R_{max} > b_K$ (see Figure 3a), the network shear modulus G_0 decreases with increasing strand Kuhn length as $b_K^{-3/2}$ (see eq 13). The opposite trend is observed for stiff networks (biological networks), $R_{max} < b_K$, shear modulus G_0 increases with increasing the chain Kuhn length (see eq 17). This explains trend observed in Figure 3b that larger deformations occur in softer networks at the same value of the applied uniaxial stress, σ_{xx}. Crossover between two different types of networks occurs at $R_{max} \approx b_K$. Note that for a very stiff networks made of chains with chain degree of polymerization $N = 20$ and bending constant $K > 300$ we see a deviation from the straight line and saturation. This

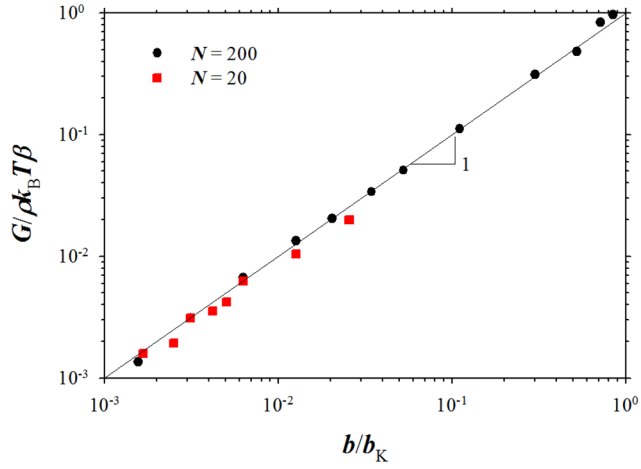

Figure 4. Dependence of the reduced shear modulus on the ratio of the bond length b to the Kuhn length b_K.

indicates a crossover to the bond stretching regime already at small network deformations, $\lambda \approx 1$. Assuming that in the linear deformation regime each bond can be approximated by an elastic spring with spring constant K_{bond}, the spring constant of the polymeric strand between cross-links K_{ch} is N_b times smaller than spring constant of individual bonds, $K_{ch} = K_{bond}/N_b$. (Note that the value of bond spring constant K_{bond} is determined by parameters of the bond potential (see Appendix A).) The shear modulus of the network of springs at small deformations can be estimated as $G_0 \approx K_{ch}/R_{max} \approx K_{bond}b/R_{max}^2$ and is independent of the chain Kuhn length, b_K. Thus, in the bond stretching regime

dx.doi.org/10.1021/ma400478f | Macromolecules 2013, 46, 3679−3692

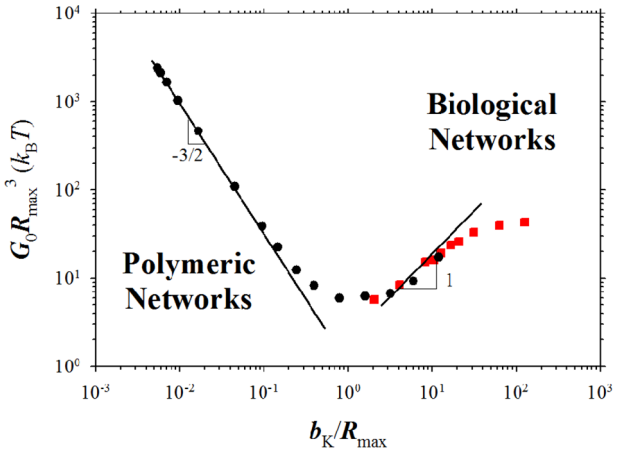

Figure 5. Dependence of the reduced shear modulus $G_0R_{max}^3$ on the ratio of the Kuhn length b_K to the fully extended chain size R_{max}.

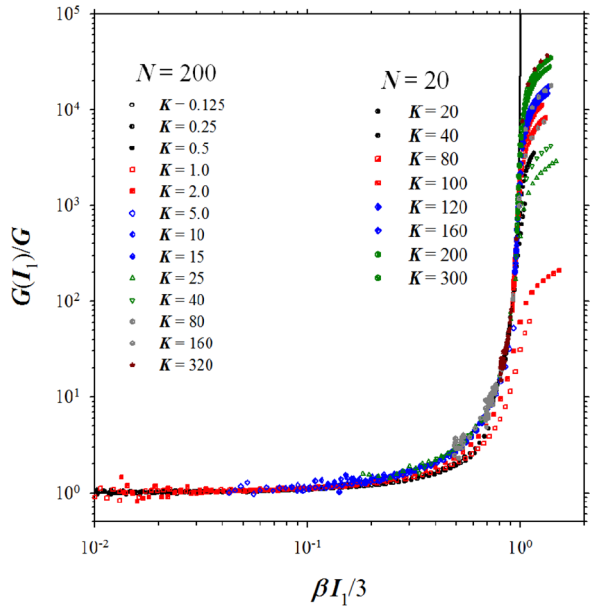

Figure 6. Dependence of the reduced network shear modulus $G(I_1)/G$ on the parameter $\beta I_1/3$ for diamond networks made of polymer chains with different bending constants K and number of monomers between cross-links N = 20 and N = 200. The solid line is given by eq 23.

network, shear modulus G_0 should become independent of the ratio b_K/R_{max} and saturate. Crossover to this regime occurs at $b_k/R_{max} \approx K_{bond}bR_{max}/k_BT$.

Note that we can use a different representation of the data shown in Figure 5 and collapse data in chain bending and bond stretching regimes as it is done for mechanical networks of filaments.[27] This data collapse is done by normalizing the network shear modulus by shear modulus in the bond stretching regime and by introducing the effective chain persistence length as $l_e \approx (E_{bend}/K_{bond})^{1/2}$. In this representation the reduced network shear modulus will be a quadratic function of l_e/R_{max} and crossover to bond stretching regime will occur at $l_e/R_{max} \propto 1$. However, this collapse of the data will come at the expense of universality in the entropic stretching regime.

To describe entire interval of network deformations we introduce a deformation dependent network shear modulus in the case of the uniaxial deformation as

$$G(I_1) \equiv \frac{\sigma_{xx}(\lambda)}{\lambda^2 - \lambda^{-1}} = \frac{G}{3}\left(3 + \frac{2b_K}{b}\sqrt{K^2 + \left(1 - \frac{\beta I_1(\lambda)}{3}\right)^{-2}} - \frac{2b_K}{b}\sqrt{K^2 + 1}\right) \quad (22)$$

Deformation dependent network shear modulus is a function of the of the strain invariant I_1 characterizing network deformation, parameter β determining the stretching ability of the strands between cross-links and chain bending constant K. These parameters characterize molecular specificity of polymeric strands forming networks. In Figure 6 we plot reduced network shear modulus, $G(I_1)/G$ as a function of the network deformation invariant and chain elongation ratio, βI_1. In the linear network deformation regime, $\beta I_1 < 1$, all data sets have collapsed into one universal plot independent of the value of the chain bending constant K. The reason for such universal behavior is that for networks made of flexible chains with $K < 1$ our data corresponds to linear network deformation regime where parameter $\beta I_1 \ll 1$ (see Figure 3). In this regime the deformation dependent network shear modulus $G(I_1)$ is equal to G. In the case of networks made of semiflexible or rigid polymeric chains eq 16 can be simplified as[33]

$$G(I_1) = \frac{G}{3}\left(1 + 2\left(1 - \frac{\beta I_1(\lambda)}{3}\right)^{-2}\right) \quad (23)$$

and it becomes a universal function of the parameter βI_1 and is independent of bending constant K. The deviation from universal behavior is observed at large network deformations for networks made of chains with $K > 1$ where individual bonds begin to stretch (see also Figure 3, parts a and b). Note that quadratic divergence of the network shear modulus at large network deformations exists even in the case of networks with $K < 5$. However, for such networks this regime is relatively narrow (see Figure 2). A crossover between eq 23 and a regime where network deformation dependent modulus demonstrates a divergence $G(I_1) \propto (1 - \beta I_1/3)^{-1}$is given by eq 20. We see this crossover for our networks with $K < 5$ which is manifested by deviation from universal curve at large network deformations, $\beta I_1 > 0.6$.

We can clearly see two different nonlinear network deformation regimes by plotting nonlinear modulus data as $G(I_1)b/(GKb_K)$ vs $K(1-\beta I_1/3)$ (see Figure 7). In the bending deformation regime, we recover a quadratic divergence. This regime is followed by the nonlinear FJC network deformation regime where $G(I) \propto (1 - \beta I_1/3)^{-1}$. Deviation from universal behavior indicates a crossover to the entropic deformation regime and the bond stretching regime. Note that this data presentation is similar to the one used to highlight different chain deformation regimes.[28]

Experimental data on deformation of biological networks[34−37] ($K \gg 1$) are usually represented by plotting differential network modulus

$$\frac{d\sigma_{xx}}{d\lambda} = (2\lambda + \lambda^{-2})G(I_1) + \frac{8}{9}\frac{G\beta}{\lambda}(\lambda^2 - \lambda^{-1})^2\left(1 - \frac{\beta I_1(\lambda)}{3}\right)^{-3} \quad (24)$$

dx.doi.org/10.1021/ma400478f | Macromolecules 2013, 46, 3679−3692

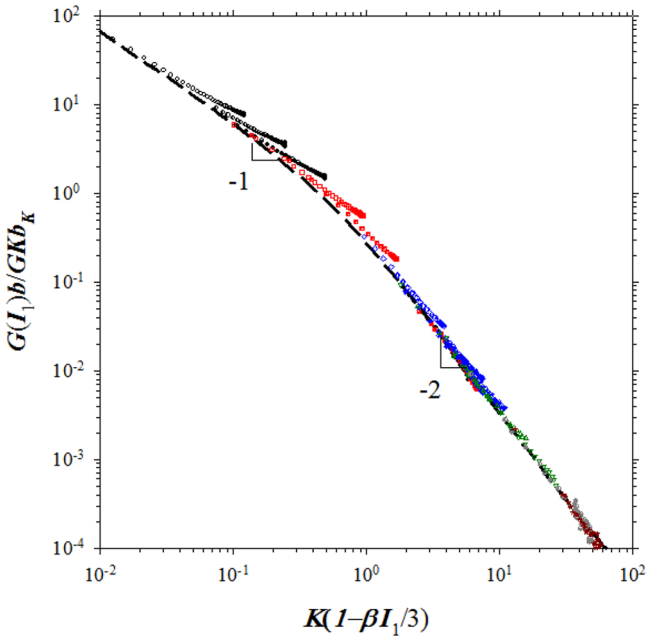

Figure 7. Dependence of the reduced network shear modulus $G(I_1)b/(GKb_K)$ on the parameter $K(1-\beta I_1/3)$ for diamond networks made of polymer chains with different bending constants K and number of monomers $N = 200$ and $N = 20$. The dashed line corresponds to numerically calculated $G(I_1)$ using eq 22 for $K = 100$. Notations are the same as in Figure 6.

as a function of the network elongational stress

$$\sigma_{xx} = \frac{G}{3}(\lambda^2 - \lambda^{-1})\left(1 + 2\left(1 - \frac{\beta I_1(\lambda)}{3}\right)^{-2}\right) \quad (25)$$

Analyzing eqs 24 and 25, one can see that it is difficult to express the divergent part of the network stress as a simple function of the stress itself in a wide interval of the network deformations ratios λ. However, it is possible to collapse data in linear and nonlinear network deformation regimes. The collapse of the data in the linear deformation regime is done by rescaling the $d\sigma_{xx}/d\lambda$ axis (y-axis). The rescaling factor is immediately obtained from the value of the differential network elongational (Young) modulus at $\lambda = 1$ which is equal to $3G_0$ (see eq 23). In the nonlinear network deformation regime we can derive dependence of the differential modulus on the applied elongational stress, σ_{xx}, by using the following arguments. For network deformation ratios $\lambda > 1$ the elongational stress, σ_{xx}, scales with the network deformation as

$$\sigma_{xx} \approx \frac{2G\lambda^2}{3}\left(1 - \frac{\beta I_1(\lambda)}{3}\right)^{-2}$$
$$\Rightarrow \left(\frac{3\sigma_{xx}}{2G}\right)^{1/2} \approx \lambda\left(1 - \frac{\beta I_1(\lambda)}{3}\right)^{-1} \quad (26)$$

Substituting this relation into expression for the differential network modulus and taking into account that in the nonlinear network deformation regime, we note that the second term in the rhs of eq 24 provides the dominant contribution and we obtain

$$\frac{d\sigma_{xx}}{d\lambda} \propto \frac{\beta}{G^{1/2}}{\sigma_{xx}}^{3/2} \quad (27)$$

Thus, in the nonlinear network deformation regime we should expect a 3/2 power law dependence of the network differential modulus on the elongation stress. Note that this scaling dependence (Table 2) is just a reflection of dominance of the

Table 2. Rescaling Parameters Used for Data Sets in Figure 8

K	G_0 (k_BT/σ^3)	${\sigma_{xx}}^*$ (k_BT/σ^3)
5	2.76×10^{-5}	2.49×10^{-4}
10	9.35×10^{-6}	5.08×10^{-5}
15	5.35×10^{-6}	2.19×10^{-5}
25	2.83×10^{-6}	8.06×10^{-6}
40	1.79×10^{-6}	3.56×10^{-6}
80	1.16×10^{-6}	1.33×10^{-6}
160	1.12×10^{-6}	7.60×10^{-7}
320	1.18×10^{-6}	5.25×10^{-7}

bending deformation modes of the individual network strands.[28,30,38] A crossover between linear and nonlinear network deformation regimes occurs at elongational stress

$$\sigma_{xx}^* \propto G^{1/3}G_0^{2/3}\beta^{-2/3} \quad (28)$$

We can use ${\sigma_{xx}}^*$ as a rescaling factor for x-axis to collapse our simulation data. This is illustrated in Figure 8 where we plotted

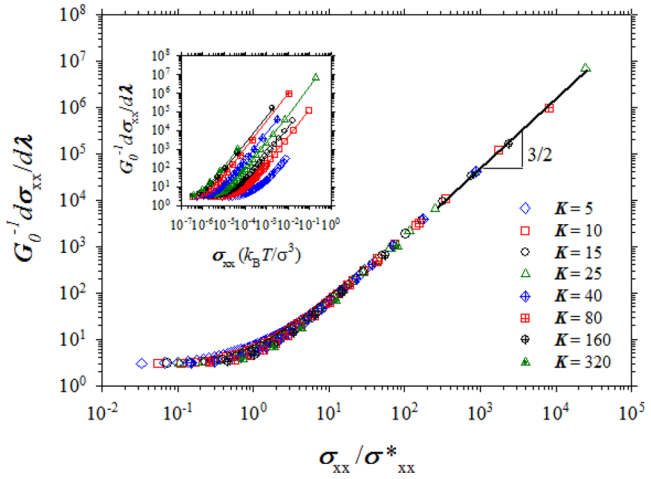

Figure 8. ${G_0}^{-1}(d\sigma_{xx}/d\lambda)$ as a function of $\sigma_{xx}/{\sigma_{xx}}^*$ for diamond networks made of semiflexible chains with different bending constants K and number of monomers $N = 200$.

simulation data for diamond networks made of chains with different values of the bending constant K. This figure clearly indicates a good collapse of the simulation data in the linear and nonlinear network deformation regimes. However in the crossover regime, $\sigma_{xx} \propto \sigma_{xx}^*$, there is a deviation from the universal behavior. In the nonlinear network deformation regime our simulation data confirm $d\sigma_{xx}/d\lambda \propto {\sigma_{xx}}^{3/2}$ scaling over the interval covering 5 orders of magnitude. This confirms scaling analysis presented above. Furthermore, our network deformation model allowed us to relate value of the crossover stress ${\sigma_{xx}}^*$ with molecular parameters of the network (see eq 28).

Nonaffinity in Network Deformation. We have shown that our model of the network elasticity derived under affine deformation assumption describes simulation data in almost entire interval of the network deformations. To establish why affine deformation model of the nonlinear network elasticity works reasonably well we will consider degree of nonaffinity in

dx.doi.org/10.1021/ma400478f | Macromolecules 2013, 46, 3679−3692

network deformation and compare macroscopic value of the first deformation matrix invariant, $I_1(\lambda) = \lambda^2 + 2/\lambda$, and its microscopic value calculated from deformation of the individual chains

$$\langle I_1(\lambda)\rangle = \frac{1}{N_{ch}}\sum_{i=1}^{N_{ch}}\left[\frac{\langle R_x^i(\lambda)^2\rangle}{(R_{p,x}^i)^2} + \frac{\langle R_y^i(\lambda)^2\rangle}{(R_{p,y}^i)^2} + \frac{\langle R_z^i(\lambda)^2\rangle}{(R_{p,z}^i)^2}\right] \tag{29}$$

where $\langle R_\alpha^i(\lambda)^2\rangle$ is the mean square value of the α th component of the end-to-end vector of the ith network strand at elongation ratio λ and $R_{p,\alpha}^i$ is the αth component of the end-to-end vector of the ith network strand in preparation state (distance between diamond network vertexes). Deviation of the average value $\langle I_1(\lambda)\rangle$ from its affine value $I_1(\lambda)$ can be considered as a measure of nonaffinity in network deformation

$$\Delta(\lambda) = \frac{\langle I_1(\lambda)\rangle}{I_1(\lambda)} - 1 \tag{30}$$

Figure 9 shows dependence of the nonaffinity parameter $\Delta(\lambda)$ as a function of the network deformation parameter $\beta I_1/3$. For

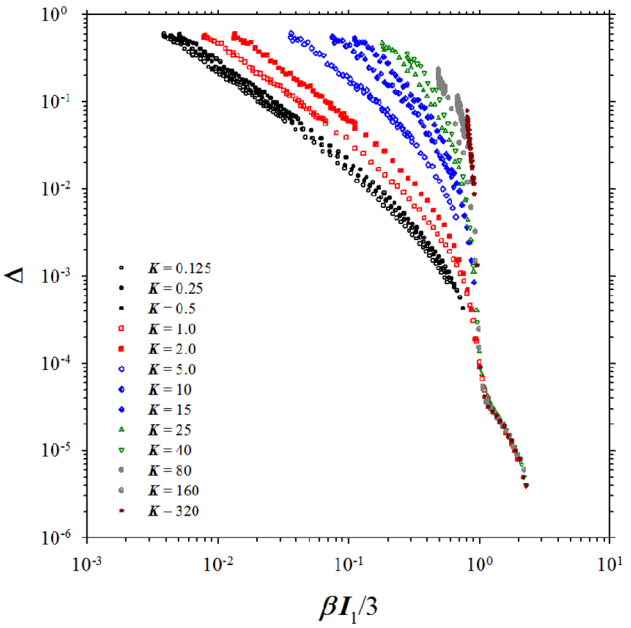

Figure 9. Dependence of the network affinity parameter $\Delta(\lambda)$ on network deformation parameter $\beta I_1/3$ for diamond networks with N = 200.

small network deformations the value of the nonaffinity parameter $\Delta(\lambda)$ is close to 0.6. This is due to fluctuations of the distance between vertexes which for flexible chains is on the order of its average value. With increasing network deformation the elongation of the polymeric strands suppresses fluctuations on the length scale of the individual strands resulting in decrease in the nonaffinity parameter $\Delta(\lambda)$. Furthermore, at $\beta I_1/3 \propto 1$ all curves converge and finally collapse to one universal curve in the bond stretching regime, $\beta I_1 > 3$. In this interval of network deformations the deformation of the individual strands is dominated by bond extension and is independent of the chain bending constant K.

It is also seen in Figure 9 that, in the wide interval of the network deformations, parameter Δ scales inversely proportional to the value of the first deformation invariant I_1. In order to explain this scaling relation, we will use a phantom network model.[20] In the framework of this model each polymer chain is attached to nonfluctuating affinely deformed background by two springs with effective spring constant K_{eff} (see Figure 10). The value of the effective spring constant K_{eff} is proportional to the elastic constant of a chain K_{ch} with proportionality coefficient C_K being function of the network structure. For tree-like networks with cross-link functionality f_n the effective spring constant $K_{\text{eff}} = K_{ch}(f_n - 2)$ and $C_K = f_n - 2$. Note that in the linear network deformation regime, $K_{ch} = 3k_BT/b_KR_{max}$. Taking this into account, one can write a mean square value of the radius vector between cross-links as follows (see Appendix B for details):

$$\langle R_\alpha^i(\lambda)^2\rangle = (\lambda_\alpha R_{p,\alpha}^i)^2 + \frac{2k_BT}{2K_{ch} + K_{eff}} \tag{31}$$

Substitution of the eq 31 into eq 29 results in

$$\langle I_1(\lambda)\rangle = I_1(\lambda) + C_{DN}\frac{b_K R_{\max}}{3R_p^{\,2}} \tag{32}$$

where numerical constant

$$C_{DN} = \frac{2}{2 + C_K}\frac{1}{N_{ch}}\sum_{i=1}\left(\frac{1}{(\cos\theta_i)^2} + \frac{1}{(\sin\theta_i\cos\phi_i\sin\phi_i)^2}\right) \tag{33}$$

depends only on the network symmetry with angles ϕ_i and θ_i describing the ith strand orientation. Thus, in the linear network deformation regime, the nonaffinity parameter Δ is equal to

$$\Delta = \frac{C_{DN}}{3}\frac{b_K R_{\max}}{R_p^{\,2} I_1} \tag{34}$$

It is inversely proportional to the magnitude of the first invariant I_1 with prefactor dependent on the bending rigidity of network strands. We can select a new normalization factor for parameter Δ and collapse all our simulation data into one universal plot by plotting $\tilde{\Delta} = \Delta R_p^{\,2}/(\beta b_K R_{\max}) \approx \Delta R_{\max}/b_K$ as a function of $\beta I_1/3$. This is shown in Figure 11. The collapse of the data is very good in the regime with $\beta I_1 < 3$, where network elasticity is controlled by deformation modes of individual network strands. However, we lose universality in the bond stretching regime where network elastic properties are determined by bond elasticity.

We can extend our analysis to the nonlinear network deformation regime by assuming that each network strand has an effective spring constant (see eq 1)

$$K_{ch} \approx \frac{3k_BT}{\langle R_0^{\,2}\rangle} + \frac{2k_BT}{R_{\max}b}\left[\sqrt{K^2 + (1 - \beta I_1/3)^{-2}} - \sqrt{K^2 + 1}\right] \tag{35}$$

where we substituted $\langle R\rangle^2$ by $\beta I_1/3$. For nonlinear springs eqs 31 and 32 can be rewritten as follows:

dx.doi.org/10.1021/ma400478f | Macromolecules 2013, 46, 3679−3692

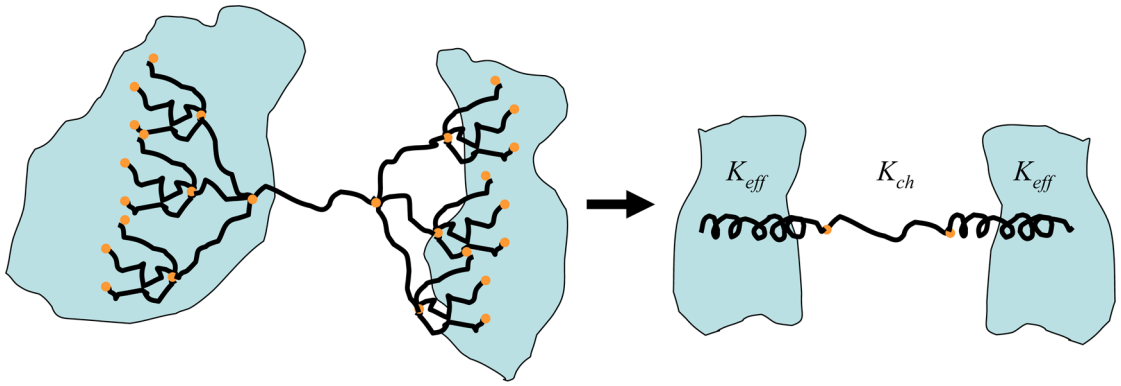

Figure 10. Schematic representation of the phantom network model.

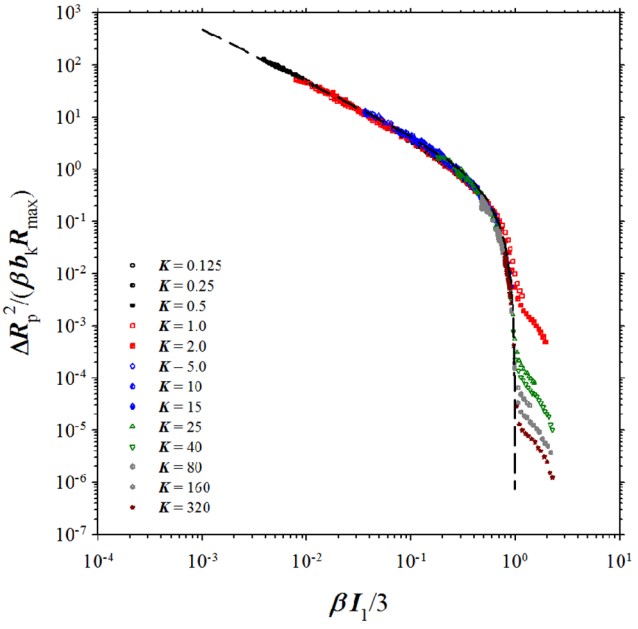

Figure 11. Dependence of the reduced network affinity parameter $\tilde{\Delta} = \Delta R_p^2/(\beta b_K R_{max})$ on the network deformation parameter $\beta I_1/3$ for diamond networks with $N = 200$. The dashed line is given by the equation $g(x) = 1.45x^{-1}(1 + 2(1 - x)^{-2})^{-1}$.

$$\Delta \approx C_{DN}\frac{b_K R_{max}}{R_p^2 I_1}\left(3 + \frac{2b_K}{b}\left[\sqrt{K^2 + (1-\beta I_1/3)^{-2}} - \sqrt{K^2+1}\right]\right)^{-1} \approx C_{DN}\frac{b_K R_{max}}{R_p^2 I_1}\frac{G}{G(I_1)} \quad (36)$$

For semiflexible networks made of chains with $K \gg 1$, eq 36 can be simplified to

$$\Delta \approx C_{DN}\frac{b_K R_{max}}{R_p^2 I_1}(1 + 2(1-\beta I_1/3)^{-2})^{-1} \quad (37)$$

This equation is shown as a dashed line in Figure 11. Collapse of the simulation data in the nonlinear network deformation regime validates our approximation of semiflexible chains by nonlinear elastic springs with effective spring constants given by eq 35.

Our analysis can also be applied to explain universality of the nonaffinity parameter Δ in the bond stretching regime, $\beta I_1 > 3$ (see Figure 10). In this regime, we can consider a polymer strand between cross-links as a sequence of N_b elastic springs connected in series each having spring constant K_{bond} (see Appendix B for detail). The spring constant of a polymer chain is $K_{ch}=K_{bond}/N_b$. Substituting this spring constant into eqs 31 and 32 we obtain for parameter Δ

$$\Delta = C_{DN}\frac{k_B T N_b}{R_p^2 K_{bond} I_1} \approx C_{DN}\frac{k_B T}{K_{bond} b^2}\frac{1}{N_b \beta I_1} \quad (38)$$

Thus, for networks with the same strand degree of polymerization N and the same values of the bond parameters K_{bond} and b the data should collapse into one universal curve. This is exactly what we see in Figure 10 for $\beta I_1 > 3$.

To conclude this section we want to stress one more time that nonaffinity in network deformation can be described in the framework of the phantom network model. In this model, the nonaffinity effects are taken into account by considering renormalized value of the network strand spring constant. This results in the change of the numerical prefactor without changing the functional form of the spring constant dependence on the network deformation. Thus, the main difference between affine and phantom network model is in a numerical prefactor, which value depends on the chemical stricture of the network such as network functionality. However, it has the same scaling dependence on the chain degree of polymerization N and chain elongation ration β. This explains why our model of nonlinear network elasticity is in a good agreement with the simulation results.

■ COMPARISON WITH EXPERIMENTS

In this section, we will apply our model to describe nonlinear deformation of polymeric and biological networks and gels.[7,36] Unfortunately, experimental studies are limited to moderate network deformations corresponding to bending deformation mode of the network strands in the nonlinear network deformation regime. To describe experimental data in linear and nonlinear network deformation regimes it is sufficient to use a simplified expression for the deformation dependent network shear modulus (see eq 23). Figure 12 combines experimental data for biological networks and gels and simulation data for diamond networks. All data sets have collapsed in to one universal plot confirming that reduced strain dependent modulus $G(I_1)/G$ is a universal function of the strain invariant I_1 characterizing network deformation and parameter β determining the stretching ability of the strands between cross-links.

dx.doi.org/10.1021/ma400478f | Macromolecules 2013, 46, 3679−3692

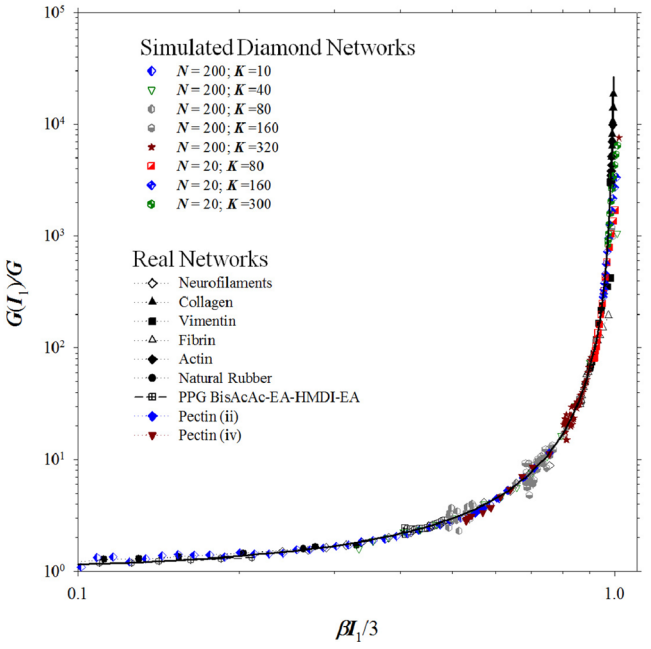

Figure 12. Dependence of the reduced network shear modulus $G(I_1)/G$ on the parameter $\beta I_1/3$ for biological and simulated networks.

The experimental values of the differential modulus are usually obtained from network shear experiments.[34−37] By using expression for the shear stress eq 9 and assuming that the main contribution to the nonlinear elastic response comes from the bending deformation mode of network strands

$$\sigma_{xy} = \frac{G\gamma}{3}\left(1 + 2\left(1 - \frac{\beta I_1(\lambda)}{3}\right)^{-2}\right) \tag{39}$$

we obtain

$$\frac{d\sigma_{xy}}{d\gamma} = G(I_1) + \frac{8}{9}G\beta\gamma^2\left(1 - \frac{\beta I_1(\gamma)}{3}\right)^{-3} \tag{40}$$

where $I_1(\gamma) = \gamma^2 + 3$ is the first strain invariant for shear deformation. At small network deformations, the differential network shear modulus is equal to $d\sigma_{xy}/d\gamma \approx G_0$. In the nonlinear network deformation regime, we can derive dependence of the differential modulus on the shear stress the same way as we did for uniaxial network deformation. This analysis results in the following expression for the differential network shear modulus

$$\frac{d\sigma_{xy}}{d\gamma} \propto \frac{\beta\gamma^{1/2}}{G^{1/2}}\sigma_{xy}^{3/2} \tag{41}$$

It follows from eq 41 that in the nonlinear network deformation regime we should expect a 3/2 power law dependence of the network differential modulus on the parameter $\gamma^{1/3}\sigma_{xy}$. Note that the power law is the same but the scaling parameter is different from what was derived for uniaxial deformation with $\lambda > 1$ and is usually used for analysis of experimental data for biological networks.[34] A crossover between linear and nonlinear network deformation regimes takes place at

$$\gamma^{*1/3}\sigma_{xy}^{*} \propto G^{1/3}G_0^{2/3}\beta^{-2/3} \Rightarrow \gamma^{*} \propto G^{1/4}G_0^{-1/4}\beta^{-1/2},$$
$$\sigma_{xy}^{*} \propto G^{1/4}G_0^{3/4}\beta^{-1/2} \tag{42}$$

We can use the parameter $\gamma^{*1/3}\sigma_{xy}^{*}$ as a rescaling factor for the x-axis to collapse experimental data for biological networks and gels. This is done in Figure 13, where we plotted experimental

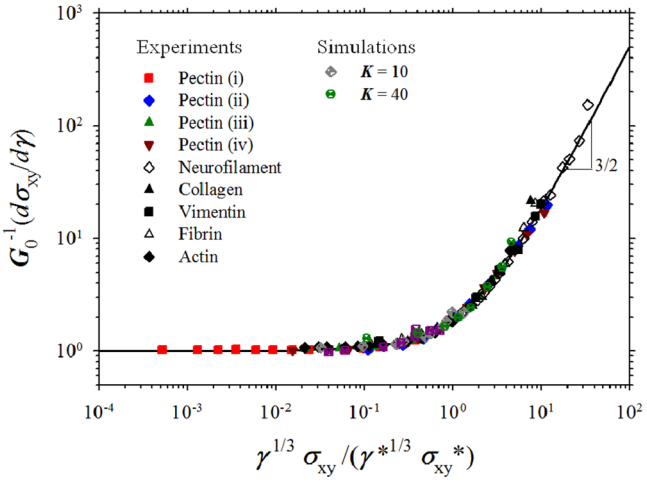

Figure 13. $G_0^{-1}(d\sigma_{xy}/d\gamma)$ as a function of $\gamma^{1/3}\sigma_{xy}/\gamma^{*1/3}\sigma_{xy}^{*}$ for biological and simulated networks. The solid line is given by a crossover equation: $y(x) = (1 + (1 + x)^{3/2})/2$.

data for biological networks of actin, fibrin, vimentin, neurofilaments, collagen,[7] and pectin.[36] The collapse of experimental data is very good. The normalization parameters used for data collapse in Figure 13 are listed in Table 3.

Table 3. Rescaling Parameters for Data Sets Used in Figure 13

	network type	G_0 (Pa)	$\gamma^{*1/3}\sigma^{*}_{xy}$ (Pa)
1	biomimetic pectin network, [PME] = 10 (fresh)[36]	1252.21	223.16
2	biomimetic pectin network, [PME] = 69 (frozen)[36]	8.76	4.44
3	biomimetic pectin network, [PME] = 25 (fresh)[36]	32.61	13.61
4	biomimetic pectin network, [PME] = 25 (frozen)[36]	46.71	18.53
5	neurofilament network[7]	1.50	3.24
6	collagen network[7]	15.98	0.53
7	vimentin network[7]	3.16	0.41
8	fibrin network[7]	18.34	3.10
9	actin network[7]	89.95	3.17
	simulated networks[33]	G_0 (k_BT/σ^3)	$\gamma^{*1/3}\sigma^{*}_{xy}$ (k_BT/σ^3)
10	K = 10, N_s = 17.90 ± 6.7, shear deformation	0.017	0.0074
11	K = 40, N_s = 17.99 ± 6.7, shear deformation	0.020	0.0046

CONCLUSIONS

We have developed a model of nonlinear network elasticity which describes network deformations in the entire interval of the applied stresses. In the framework of our model elongational and shear network stresses (see eqs 8 and 9) are functions of the first deformation invariant I_1, network strand's extensibility parameter β, strand's bending constant K and network shear modulus, G. Note that all molecular parameters associated with network preparation conditions and cross-link functionality are included into expression for the network shear modulus. There

dx.doi.org/10.1021/ma400478f | Macromolecules 2013, 46, 3679−3692

are three main modes of the network deformation: entropic stretching, network strand's bending and bond stretching (see Figure 2). These different network deformation modes are manifestations of the deformation modes of polymeric chains making up the network. Crossover between network deformation regimes depends on the chain bending constant K and deformation parameter βI_1.

In the linear deformation regime network, the shear modulus first decreases with increasing chain Kuhn length, $G_0 \propto k_BT(b_KR_{max})^{-3/2}$, then it begins to increase, $G_0 \propto k_BTb_K/R_{max}^4$ (see Figure 5). The first regime corresponds to polymeric networks made of flexible chains with $b_K < R_{max}$ while the second regime is representative of rigid (biological) networks consisting of stiff filaments, $b_K > R_{max}$. Crossover between two different network deformation regimes occurs at $b_K \approx R_{max}$. At this point network shear modulus has its minimal possible value, $G_0 \propto k_BT/R_{max}^3$. The different power law dependences of the network shear modulus on the Kuhn length is a result of different network deformation modes. For networks made of flexible chains the network elasticity is due to stretching of network strands and is entropic in nature while for rigid networks the chain bending controls network elastic response. For a very stiff networks the strand bending becomes energetically unfavorable and networks deform by stretching individual bonds. This is manifested in saturation of the networks shear modulus as a function of the Kuhn length, $G_0 \approx k_{bond}b/R_{max}^2$ (see Figure 5). In this deformation regime network elastic response is similar to that of mechanical networks of filaments.[27]

At large network deformations there are two nonlinear network deformation regimes. In the first regime strain dependent network shear modulus demonstrate a quadratic divergence, $G(I_1) \propto (1 - \beta I_1/3)^{-2}$ (see Figures 6 and 7). In this regime network strands behave as worm-like chains under tension. This result is in agreement with a simplified model of nonlinear network elasticity based on deformation of worm-like chain.[33] At larger network deformations when strand stretching occurs at the length scales much smaller than the strand Kuhn length or for networks made of flexible polymer chains the strain dependent network shear modulus has a hyperbolic divergence, $G(I_1) \propto (1 - \beta I_1/3)^{-1}$. This hyperbolic divergence of the strain dependent shear modulus is due to finite strands extensibility and reflects divergence of the chain tension characteristic of the freely jointed chain model. Therefore, at such deformations network strands behave as freely jointed chains. This is a new scaling regime which was not identified in ref 33. Crossover between these two network deformation regimes is determined by chain bending rigidity K (see Figure 2).

Nonaffinity in network deformation on the length scales of individual chains was analyzed by comparing microscopic and macroscopic values of the first deformation invariant I_1 (see eqs 29, 30) Analysis of the simulation data has shown that nonaffinity in network deformation is due to fluctuations of the cross-linking point.[20,39] This was confirmed by using a phantom network model and describing each network strand as being attached to nonfluctuating network background by two effective springs that values depend on the network functionality (see Figure 10).[39] By using the expression for the nonlinear chain spring constant (eq 35), we have been able to collapse all our simulation data for nonaffinity parameter (see Figure 9) into one universal plot in both linear and nonlinear network deformation regimes (see Figure 11). This proves that polymeric strands of the network can be described by nonlinear springs with deformation dependent spring constant. The nonaffinity in network deformation can be introduced into our model by renormalizing chain spring constant as it is done in the phantom network model. Note that the difference between affine and phantom network models only appears in the expression for the network shear modulus. Thus, all nonaffinity related factors can be absorbed into definition of the network shear modulus G. In our analysis of the stress/strain data obtained from molecular dynamics simulations (see Figure 3, parts a and b), we used network shear modulus as a fitting parameter and these corrections have already been included into network shear modulus G.

The final point that we want to make here is that our model of network elasticity does not take into account effect of entanglements.[1,20,39,40] Thus, it could only be applied to networks with chain's degree of polymerizations below entanglement molecular weight M_e. Consideration of entanglements should modify expression for the network free energy and change its functional form as a function of the strain invariant I_1. The discussion of this topic is beyond the scope of the paper.

APPENDIX A: SIMULATION DETAILS

We have performed molecular dynamics simulations[41] of deformation of networks of flexible and semiflexible chains. Chains forming a network were modeled by bead−spring chains consisting of monomers with diameter σ. The connectivity of beads in polymer chains and the cross-link bonds were described by the finite extension nonlinear elastic (FENE) potential,

$$U_{FENE}(r) = -0.5k_sR_m^2 \ln\left(1 - \frac{r^2}{R_m^2}\right) \quad \text{(A.1)}$$

where k_s is the spring constant set to $k_s = 100k_BT/\sigma^2$, the maximum bond length is $R_m = 1.5\sigma$, k_B is the Boltzmann constant and T is the absolute temperature. (The large value of the spring constants was selected to minimize the effect of the bond stretching at large network deformations). The repulsive part of the bond potential was modeled by the shifted Lennard-Jones potential with the values of the Lennard-Jones interaction parameter $\varepsilon_{LJ} = 1.5\ k_BT$. The chain bending rigidity was introduced into the model through a bending potential controlling the mutual orientations between two neighboring along the polymer backbone unit bond vectors $\vec{n}_i$ and $\vec{n}_{i+1}$

$$U_{i,i+1}^{bend} = k_BTK(1 - (\vec{n}_i \cdot \vec{n}_{i+1})) \quad \text{(A.2)}$$

In our simulations the value of the bending constant K was varied between 0.125 and 1200. For this chain model a chain Kuhn length b_K is related to the chain's bending constant K through eq 2, where $b = 0.90 \pm 0.01\ \sigma$ is the bond length. We did not have any additional interactions between monomers. The network had structure of the diamond network (see Figure 14).

Simulations were carried out in a constant number of particles, and temperature ensemble. The constant temperature was maintained by coupling the system to a Langevin thermostat. In this case, the equation of motion of ith bead is

$$m\frac{d\vec{v}_i(t)}{dt} = \vec{F}_i(t) - \xi\vec{v}_i(t) + \vec{F}_i^R(t) \quad \text{(A.3)}$$

where $\vec{v}_i(t)$ is the ith bead velocity, and $\vec{F}_i(t)$ is the net deterministic force acting on ith bead with mass m. $\vec{F}_i^R(t)$ is the stochastic force with zero average value $\langle\vec{F}_i^R(t) = 0\rangle$ and δ-functional correlations $\langle\vec{F}_i^R(t)\vec{F}_i^R(t')\rangle = 6\xi k_BT\delta(t - t')$. The friction coefficient ξ was set to $\xi = 0.25\ m/\tau_{LJ}$, where τ_{LJ} is the

dx.doi.org/10.1021/ma400478f | Macromolecules 2013, 46, 3679−3692

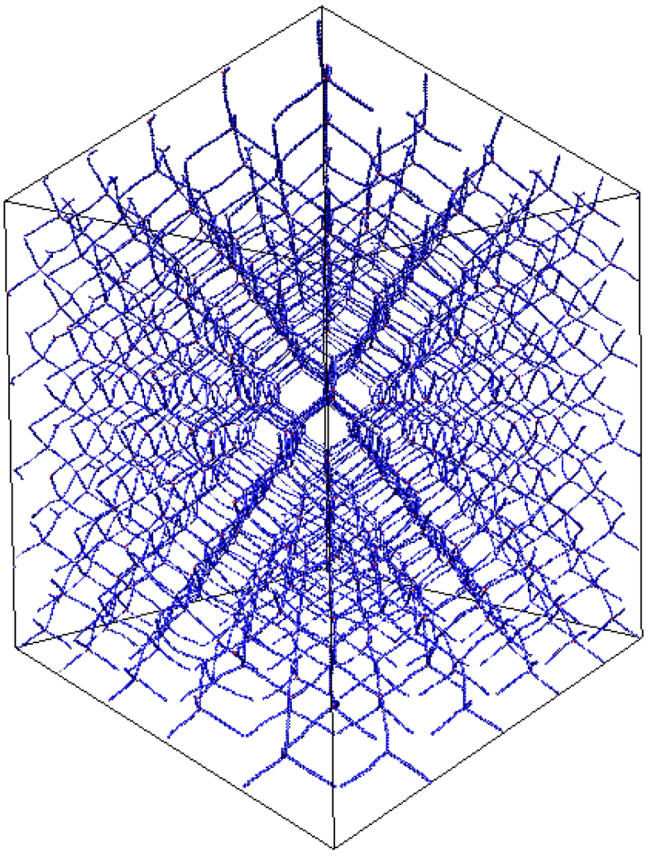

Figure 14. Diamond network of polymer chains with number of monomers $N = 20$.

standard LJ-time $\tau_{LJ} = \sigma(m/\varepsilon_{LJ})^{1/2}$. The velocity−Verlet algorithm with a time step $\Delta t = 0.005\tau_{LJ}$ was used for integration of the equations of motion (eq A.3). All simulations were performed using LAMMPS.[42] We have performed simulations of two different types of networks. In network of the first type each polymer strand between cross-links had $N = 200$ monomers (Table 4) while in the networks of the second type we only had $N = 20$. This allowed us to cover five orders in b_K/R_{max} ratios (see Figure 5).

Table 4. Simulation Values

N	no. of vertices	no. of beads
200	64	25 408
20	1000	37 000

In order to obtain stress−strain relation for diamond networks of chains we have performed sets of simulations of uniaxial network deformations. The networks were deformed by changing the initial box size L_0 along the x direction to λL_0 and to $L_0/\sqrt{\lambda}$ in the y and z directions.[40] Under such deformation the system volume remained the same. This deformation was achieved by a series of small affine deformations $\{x_i, y_i, z_i\} \rightarrow \{\Delta\lambda x_i, y_i/\Delta\lambda^{1/2}, z_i/\Delta\lambda^{1/2}\}$ until the desired strain was obtained. The molecular dynamics simulation proceeded during the constant-volume deformation process such that the network was allowed to adjust its conformations for 10^7 integration steps. The final 5×10^6 integration steps we used for the data averaging. The stress σ_{xx} in the direction of the strain was evaluated from the simulations through the pressure tensor P_{ij} as follows

$$\sigma_{xx} = \frac{3}{2}P_{xx} - \frac{1}{2}\sum_i P_{ii} \tag{A.4}$$

APPENDIX B: FLUCTUATIONS OF THE NETWORK STRAND SIZE

In this appendix, we present a generating function method for calculation of the mean square value of the end-to-end distance of polymeric strands between cross-links in the framework of the phantom network model.[20,39,43] In this model to account for fluctuations of the cross-linking points each network strand is attached to nonfluctuating background by two springs with spring constants equal to K_{eff}.

Let us consider a one-dimensional sequence of three springs with spring constants K_{eff} and K_{ch} (see Figure 15). The ends of

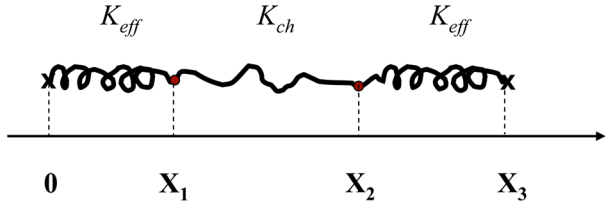

Figure 15. Series of three springs.

the spring assembly are fixed at the origin and at X_3. While two middle points X_1 and X_2 are allowed to fluctuate. The probability distribution function of the location of the points X_1 and X_2 is given by

$$P(X_1, X_2|X_3) \propto \exp\left[-\frac{K_{eff}}{2k_BT}X_1^2 - \frac{K_{ch}}{2k_BT}(X_2 - X_1)^2 - \frac{K_{eff}}{2k_BT}(X_3 - X_2)^2\right] \tag{B.1}$$

The mean square value of the distance between points X_1 and X_2 (end-to-end distance), $\langle(X_2 - X_1)^2\rangle$, is a second moment of the distribution function

$$\langle(X_2 - X_1)^2\rangle = \frac{\int_{-\infty}^{\infty} dX_1 \int_{\infty}^{\infty} dX_2\ (X_2 - X_1)^2 P(X_1, X_2|X_3)}{\int_{-\infty}^{\infty} dX_1 \int_{\infty}^{\infty} dX_2\ P(X_1, X_2|X_3)} \tag{B.2}$$

In order to perform integrations in eq B.2 it is convenient to introduce generating function

$$Z(X_3) = \int_{-\infty}^{\infty} dX_1 \int_{\infty}^{\infty} dX_2 \int_{-\infty}^{\infty} dX\ \delta(X - X_3)\ P(X_1, X_2|X) \tag{B.3}$$

where $\delta(x)$ is a delta function. The mean square value of the end-to-end distance $\langle(X_2 - X_1)^2\rangle$is obtained by differentiating generating function $Z(X_3)$ with respect to K_{ch}

$$\langle(X_2 - X_1)^2\rangle = -\frac{2k_BT}{Z(X_3)}\frac{\partial Z(X_3)}{\partial K_{ch}} \tag{B.4}$$

In order to obtain generating function $Z(X_3)$ as a function of spring constant K_{ch}, we use an integral representation of the delta function

dx.doi.org/10.1021/ma400478f | Macromolecules 2013, 46, 3679−3692

$$\delta(X - X_2) = \frac{1}{2\pi}\int_{-\infty}^{\infty} dq\, \exp(iq(X - X_2)) \tag{B.5}$$

and change variables X_1, X_2, $X \to X_1$, $X_2 - X_1$, and $X - X_2$. After these transformations integrations in eq B.3 are reduced to calculation of four Gaussian integrals resulting in

$$Z(X_3) = 2\pi k_B T \frac{\hat{K}^{1/2}}{K_{eff} K_{ch}^{1/2}} \exp\left(-\frac{\hat{K} X_3^2}{2k_B T}\right) \tag{B.6}$$

where

$$\hat{K}^{-1} = 2K_{eff}^{-1} + K_{ch}^{-1} \tag{B.7}$$

is effective spring constant of three springs connected in series. Performing differentiation of eq B.6 with respect to spring constant K_{ch} and substituting this expression into eq B.4 we have

$$\langle (X_2 - X_1)^2 \rangle = \frac{K_{eff}^2}{(2K_{ch} + K_{eff})^2} X_3^2 + \frac{2k_B T}{(2K_{ch} + K_{eff})} \tag{B.8}$$

The first term is the square of the average value of the end-to-end distance $\langle X_2 - X_1 \rangle$ while the second term describes its fluctuations.

In the case of the three-dimensional network we have to consider fluctuations of the end-to-end distance of the network strands along x, y, and z directions. Note that we can also relate the average value of the strand end-to-end distance with the distance between vertices of the diamond network in preparation condition, $R^i_{p,\alpha}$, by taking into account its affine deformation. In this case eq B.8 reduces to

$$\langle R^i_\alpha(\lambda)^2 \rangle = (\lambda_\alpha R^i_{p,\alpha})^2 + \frac{2k_B T}{2K_{ch} + K_{eff}} \tag{B.9}$$

where $\langle R^i_\alpha(\lambda)^2 \rangle$ is the mean square value of the α th component of the end-to-end vector of the ith network strand at elongation ratio λ and $\langle R^i_{p,\alpha} \rangle$ is α th component of the end-to-end vector of the ith network strand in preparation state (distance between diamond network vertexes) .

We can extend analysis presented above to the case of large network deformations when individual bonds begin to stretch, $\beta I_1 > 3$. In this case eq B.1 should be written for fluctuations of the end-to-end distance rather than for distances itself. In the fully extended conformation a polymer chain can be considered as a set of N_b bonds with harmonic bond constant, K_{bond}, connected in series. The polymer chain spring constant K_{ch} for this bond configuration is equal to

$$K_{ch} = K_{bond}/N \tag{B.10}$$

The individual bond constant is calculated as the second derivative of the bond potential

$$K_{bond} \approx \left.\frac{\partial^2 U_{bond}(r)}{\partial r^2}\right|_{r=\langle r_b^2 \rangle^{1/2}} \tag{B.11}$$

where $\langle r_b^2 \rangle$ is the mean square average bond length. This value can be related to the first deformation invariant and undeformed bond length b

$$\langle r_b^2 \rangle \approx \frac{\langle R^2 \rangle}{N^2} \approx \frac{(\lambda^2 + 2/\lambda)}{3} \frac{R_p^2}{N^2} = b^2 \frac{\beta I_1}{3} \tag{B.12}$$

such that, at crossover to the bond stretching regime, the average bond length is equal to b. In our simulations the bond potential was approximated by the sum of the FENE and truncated-shifted LJ-potential (see Appendix A).

$$U_{bond}(r) = U_{FENE}(r) + U_{LJ}(r) \tag{B.13}$$

Thus, taking second derivative and substituting value of $\langle r_b^2 \rangle$ (see eq B.12) one can obtain an expression for the bond constant as a function of the deformation invariant, I_1.

AUTHOR INFORMATION

Corresponding Author

*E-mail: avd@ims.uconn.edu.

Notes

The authors declare no competing financial interest.

ACKNOWLEDGMENTS

This work was supported by the National Science Foundation under Grant DMR-1004576. The authors would like to thank Prof. M. Williams and Dr. E. Schuster for providing experimental data on pectin networks.

REFERENCES

(1) Treloar, L. R. G., *The Physics of Rubber Elasticity*. Clarendon Press: Oxford, U.K., 2005.

(2) Torres, F. G.; Troncoso, O. P.; Lopez, D.; Grande, C.; Gomez, C. M. Reversible stress softening and stress recovery of cellulose networks. *Soft Matter* **2009**, *5*, 4185−4190.

(3) Trepat, X.; Deng, L. H.; An, S. S.; Navajas, D.; Tschumperlin, D. J.; Gerthoffer, W. T.; Butler, J. P.; Fredberg, J. J. Universal physical responses to stretch in the living cell. *Nature* **2007**, *447*, 592−595.

(4) Trepat, X.; Lenormand, G.; Fredberg, J. J. Universality in cell mechanics. *Soft Matter* **2008**, *4*, 1750−1759.

(5) Kasza, K. E.; Rowat, A. C.; Liu, J. Y.; Angelini, T. E.; Brangwynne, C. P.; Koenderink, G. H.; Weitz, D. A. The cell as a material. *Curr. Opin. Cell Biol.* **2007**, *19*, 101−107.

(6) Weisel, J. W. Biophysics—Enigmas of blood clot elasticity. *Science* **2008**, *320*, 456−457.

(7) Storm, C.; Pastore, J. J.; MacKintosh, F. C.; Lubensky, T. C.; Janmey, P. A. Nonlinear elasticity in biological gels. *Nature* **2005**, *435*, 191−194.

(8) Discher, D. E.; Janmey, P.; Wang, Y. L. Tissue cells feel and respond to the stiffness of their substrate. *Science* **2005**, *310*, 1139−1143.

(9) Franceschini, G.; Bigoni, D.; Regitnig, P.; Holzapfel, G. A. Brain tissue deforms similarly to filled elastomers and follows consolidation theory. *J. Mech. Phys. Sol.* **2006**, *54*, 2592−2620.

(10) Becker, G. W.; Kruger, O. On the nonlinear biaxial stress-strain behavior of rubberlike polymers. In *Deformation and Fracture of High Polymers*; Kausch, H. H., Hessell, J. A., Jaffee, R. I., Eds.; Plenum Press: New York, 1972.

(11) Arruda, E. M.; Boyce, M. C. A 3-dimensional constitutive model for the large strength behavior of rubber elastic materials. *J. Mech. Phys. Sol.* **1993**, *41*, 389−412.

(12) Boyce, M. C.; Arruda, E. M. Constitutive models of rubber elasticity: A review. *Rubber Chem. Technol.* **2000**, *73*, 504−523.

(13) Lin, Y. C.; Koenderink, G. H.; MacKintosh, F. C.; Weitz, D. A. Control of non-linear elasticity in F-actin networks with microtubules. *Soft Matter* **2011**, *7*, 902−906.

(14) Gardel, M. L.; Kasza, K. E.; Brangwynne, C. P.; Liu, J. Y.; Weitz, D. A. Mechanical Response of Cytoskeletal Networks. In *Biophysical Tools for Biologists, Vol 2: In Vivo Techniques*; Academic Press: San Diego, CA, 2008; Vol. *89*, p 487.

(15) Huisman, E. M.; van Dillen, T.; Onck, P. R.; Van der Giessen, E. Three-dimensional cross-linked F-actin networks: Relation between network architecture and mechanical behavior. *Phys. Rev. Lett.* **2007**, *99*, 208103.

(16) Janmey, P. A.; Georges, P. C.; Hvidt, S. Basic rheology for biologists. In *Cell Mechanics*, **2007**; Vol. *83*, pp 3−27.
(17) Janmey, P. A.; Winer, J. P.; Weisel, J. W. Fibrin gels and their clinical and bioengineering applications. *J. R. Soc. Int.* **2009**, *6*, 1−10.
(18) MacKintosh, F. C. Elasticity and dynamics of cytoskeletal filaments and their networks. In *Soft condensed matter physics in molecular and cell biology*; Poon, W. C. K., Andelman, D., Eds.; Taylor & Francis: New York, 2006; pp 139−155.
(19) Broedersz, C. P.; Kasza, K. E.; Jawerth, L. M.; Munster, S.; Weitz, D. A.; MacKintosh, F. C. Measurement of nonlinear rheology of cross-linked biopolymer gels. *Soft Matter* **2010**, *6*, 4120−4127.
(20) Rubinstein, M.; Colby, R. H., *Polymer Physics*. Oxford University Press: New York, 2003.
(21) Satcher, R. L.; Dewey, C. F. Theoretical estimates of mechanical properties of the endothelial cell cytoskeleton. *Biophys. J.* **1996**, *71*, 109−118.
(22) Kroy, K.; Frey, E. Force-extension relation and plateau modulus for wormlike chains. *Phys. Rev. Lett.* **1996**, *77*, 306−309.
(23) Mackintosh, F. C.; Kas, J.; Janmey, P. A. Elasticity of semiflexible biopolymer networks. *Phys. Rev. Lett.* **1995**, *75*, 4425−4428.
(24) Kroy, K. Elasticity, dynamics and relaxation in biopolymer networks. *Curr. Opin. Colloid Interface Sci.* **2006**, *11*, 56−64.
(25) Hatami-Marbini, H.; Picu, R. C. Scaling of nonaffine deformation in random semiflexible fiber networks. *Phys. Rev. E* **2008**, *77*, 062103.
(26) Broedersz, C. P.; Mao, X. M.; Lubensky, T. C.; MacKintosh, F. C. Criticality and isostaticity in fibre networks. *Nature Physics* **2011**, *7*, 983−988.
(27) Broedersz, C. P.; Sheinman, M.; MacKintosh, F. C. Filament-length-controlled elasticity in 3D fiber networks. *Phys. Rev. Lett.* **2012**, *108*, 108078102.
(28) Dobrynin, A. V.; Carrillo, J.-M. Y.; Rubinstein, M. Chains are more flexible under tension. *Macromolecules* **2010**, *43*, 9181−9190.
(29) Fixman, M.; Kovac, J. Polymer conformational statistics. III. Modified Gaussian model of stiff chains. *J. Chem. Phys.* **1973**, *58*, 1564.
(30) Marko, J. F.; Siggia, E. D. Stretching DNA. *Macromolecules* **1995**, *28*, 8759−8770.
(31) Livadaru, L.; Netz, R. R.; Kreuzer, H. J. Stretching response of discrete semiflexible polymers. *Macromolecules* **2003**, *36*, 3732−3744.
(32) Bustamante, C.; Smith, S. B.; Liphardt, J.; Smith, D. Single-molecule studies of DNA mechanics. *Curr. Opin. Struc. Biol.* **2000**, *10*, 279−285.
(33) Dobrynin, A. V.; Carrillo, J.-M. Y. Universality in nonlinear elasticity of biological and polymeric networks and gels. *Macromolecules* **2011**, *44*, 140−146.
(34) Gardel, M. L.; Shin, J. H.; MacKintosh, F. C.; Mahadevan, L.; Matsudaira, P.; Wietz, D. A. Elastic Behavior of Cross-Linked and Bundled Actin Networks. *Science* **2004**, *304*, 1301−1305.
(35) Gardel, M. L.; Nakamura, F.; Hartwig, J. H.; Crocker, J. C.; Stossel, T. P.; Weitz, D. A. Prestressed F-actin networks cross-linked by hinged filamins replicate mechanical properties of cells. *Proc. Natl. Acad. Sci. U.S.A.* **2006**, *103*, 1762−1767.
(36) Schuster, E.; Lundin, L.; Williams, M. A. K. Investigating the Relationship between Network Mechanics and Single-Chain Extension Using Biomimetic Polysaccharide Gels. *Macromolecules* **2012**, *45*, 4863−4869.
(37) Kasza, K. E.; Koenderink, G. H.; Lin, Y. C.; Broedersz, C. P.; Messner, W.; Nakamura, F.; Stossel, T. P.; MacKintosh, F. C.; Weitz, D. A. Nonlinear elasticity of stiff biopolymers connected by flexible linkers. *Phys Rev E* **2009**, *79*, 041928.
(38) Odijk, T. Stiff chains and filaments under tension. *Macromolecules* **1995**, *28*, 7016−7018.
(39) Rubinstein, M.; Panyukov, S. Elasticity of polymer networks. *Macromolecules* **2002**, *35*, 6670−6686.
(40) Grest, G. S.; Putz, M.; Everaers, R.; Kremer, K. Stress-strain relation of entangled polymer networks. *J. Non-Cryst. Sol.* **2000**, *274*, 139−146.
(41) Frenkel, D.; Smit, B., *Understanding Molecular Simulations*; Academic Press: New York, 2002.
(42) Plimpton, S. J. Fast parallel algorithms for short-range molecular dynamics *J. Comput. Phys.* **1995**, *117*, 1−19.
(43) Higgs, P. G.; Ball, R. C. Polydisperse polymer networks: elasticity, orientational properties, and small angle neutron scattering. *J. Phys. (Paris)* **1988**, *49*, 1785−1811.